Scanning near-field optical microscope using an atomic force microscope cantilever with integrated photodiode

Scanning near-field optical microscope using an atomic force microscope cantilever with integrated photodiode

S. Akamine[a] and H. Kuwano
NTT Interdisciplinary Research Laboratories, 9-11-3 Midori-Cho, Musashino, Tokyo 160, Japan

H. Yamada[b]
National Institute for Advanced Interdisciplinary Research, 1-1-4 Higashi, Tsukuba, Ibaraki 305, Japan

(Received 13 July 1995; accepted for publication 16 November 1995)

A combined atomic force and scanning near-field optical microscope is presented. The critical component of the instrument is a single crystal silicon, microfabricated force-sensing cantilever with an integrated photodiode. Near-field optical images are obtained by monitoring variations in the optical power detected by the photodiode while the cantilever tip is scanned in an evanescent optical field created by illuminating the sample by total internal reflection. Near-field optical power was detected at tip-sample spacings of one-quarter wavelength. Atomic force and scanning near-field optical microscope images of the same samples show corresponding features as small as 25 nm. © *1996 American Institute of Physics.* [S0003-6951(96)01305-2]

While traditional optical microscopy is limited by diffraction, resolution beyond the diffraction limit is possible by detecting higher spatial frequency optical components which exist only within fractions of a wavelength above a sample surface.[1–3] Scanning near-field optical microscopes (SNOM), with resolutions as high as 12 nm (Ref. 4) have been demonstrated. Two remaining difficulties associated with SNOM involve the development of an easily manufacturable SNOM probe and the addition of a reliable independent feedback mechanism for controlling the gap spacing between probe and sample. The most common SNOM probe is a sharpened optical fiber coated with metal except at its apex where an aperture of a few tens of nanometers is formed.[4,5] However, the process does not lend itself to mass manufacturing in contrast to atomic force microscope (AFM) cantilevers.[6] Also, while apertures in the metal film can be made 20 nm or smaller, the effective tip radius is determined by the thickness of the metal film, usually approximately 100 nm;[4] therefore, the outer diameter of the optical fiber probe is approximately 200 nm. Another unresolved difficulty of SNOM is the need to incorporate a non-optical mechanism that can control the tip-sample spacing. The need for an independent feedback mechanism arises because the optical signal is modulated not only by changes in the tip-sample spacing but also by the local optical properties of the sample. Typical non-optical methods of feedback include dithering the tip laterally to detect shear forces[7] or bending the end of the fiber itself to create a spring structure resembling the AFM cantilever.[8]

An elegant SNOM instrument that eliminates the need for an optical fiber and readily allows for the detection of forces has been demonstrated by van Hulst *et al.*[9] They use a silicon nitride AFM cantilever with a pyramidal tip.[6] Near-field optical images are obtained by bringing the tip close to the sample surface allowing it to scatter some of the light from the non-propagating evanescent fields into propagating modes that are then collected using a standard optical objective. In this configuration, the deflection of the cantilever can be monitored readily by the optical lever method common in AFM.

We have modified van Hulst's configuration by fabricating a silicon AFM cantilever with an integral photodetector, referred to as a photocantilever. The presence of the detector on the cantilever obviates the need for external optical components rendering the instrument smaller and less susceptible to mechanical vibrations (Fig. 1).

The SNOM probe is a single crystal silicon cantilever fabricated using an integrated circuit microfabrication processes.[6,10,11] Each cantilever is approximately 1000 μm in length, 200 μm in width, and 5 μm in thickness (Fig. 2). The photodiode is a simple p-n junction at the apex of the cantilever. Although silicon p-n junctions can have quantum efficiencies of approximately 90% for 670 nm wavelength radiation, the light penetration depth in silicon is 5 μm.[12] Therefore, the cantilever was designed to be substantially thicker than the 0.5 to 1 μm typical of commercially available silicon nitride cantilevers in order to allow maximum light absorption. By choosing a cantilever thickness of 5 μm

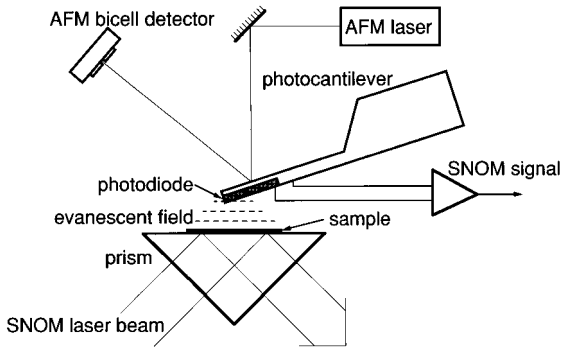

FIG. 1. Experimental setup for SNOM combined with AFM using a silicon cantilever with an integrated photodiode (photocantilever).

[a]Present address: P.O. Box 7704, Stanford, CA 94309.
[b]Author to whom correspondence should be addressed. Electronic mail: yamada@nrlm.go.jp

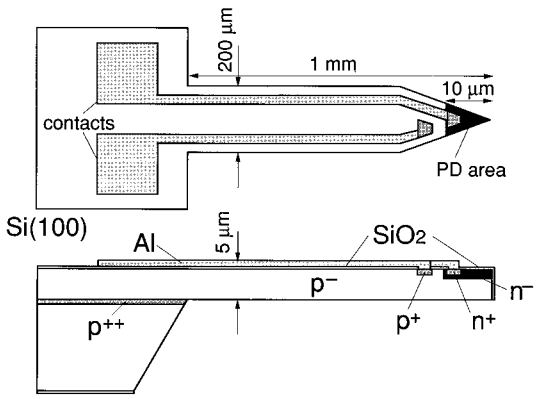

FIG. 2. Schematic drawing of a photocantilever. Plane view (up) and cross section (bottom).

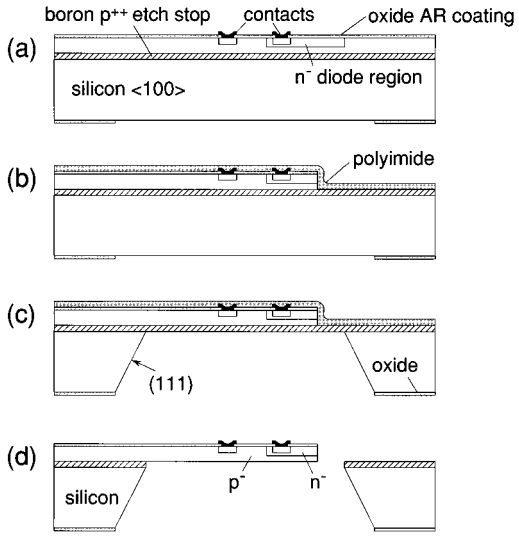

FIG. 3. Fabrication process for photocantilevers.

however, it was necessary to make cantilevers 500 to 2000 μm in length to obtain force constants in a desired range near 1 N/m.

The fabrication sequence for the photosensitive AFM cantilever is similar to a process for making piezoresistive AFM cantilevers.[10] The staring substrate for our device is a 4 in. lightly doped p-type silicon wafer. Silicon epitaxy is used to grow an etch stop layer as well as a lightly doped layer used for fabrication of electronic devices. The etch stop layer is 1 μm thick and doped to 3×10^{20} cm^{-3} with boron and germanium. Germanium is included to reduce the residual stress caused by the mismatch of lattice constants of silicon and boron.[13] A 5 μm thick layer of 3×10^{15} cm^{-3} boron doped silicon is grown over the etch stop layer. The p-n junction photodiode is fabricated by ion implanting 10^{18} cm^{-3} phosphorus into the lightly doped p-type surface epitaxy layer. The cross section of the photodiode is approximately 50 μm^2. The wafer is then thermally oxidized to create an oxide film which serves as both an antireflection coating for the photodiode as well as a passivation layer. Windows are patterned in the back side of the wafer for the final stages of the process to completely etch away the silicon under the cantilevers to yield free-standing structures; 500 nm of aluminum are then sputtered on the wafer and patterned into contact pads and metal lines [Fig. 3(a)]. Next, the actual shape of the cantilever is created by patterning a 6 μm thick film of AZ 4620 photoresist. In order to free the cantilever from the substrate, the front of the wafer is coated with approximately 50 μm of Hitachi PIX3500 polyimide [Fig. 3(b)]. The wafer is then etched in EDP at 105 °C until the etch stop layer is reached, leaving 5 μm thick cantilevers resting on 1 μm thick silicon membranes [Fig. 3(c)]. The silicon membranes are removed by dry etching from the back side. The polyimide film is removed in an oxygen plasma [Fig. 3(d)]. For simplicity, the present cantilevers do not have specially fabricated tips. Once the photocantilever probes are completed, they are placed in an optical beam deflection-type AFM designed by the authors.

In order to demonstrate that the photocantilever can detect light from evanescent fields, a prism sample was illuminated with light from a 70 μW He–Ne laser at an angle of total internal reflection. The cantilever was brought into contact with the surface repeatedly while variations in detected optical power versus the tip displacement were recorded. A typical optical power versus distance curve is shown in Fig. 4. At large tip-sample separations (left), the detected optical signal is low and does not vary with changes in spacing. At approximately 150 nm above the surface of the sample however, in the presence of the evanescent field, the detected optical signal rises sharply and saturates at approximately 12 nW (Fig. 4). Once the cantilever contacts the surface, contamination holds the cantilever until a restoring force is reached at which point the cantilevers ''snap back'' from the surface. The measured decay length of the evanescent field is approximately 150 nm, which is in good agreement with the theoretical value. The 12 nW detected at saturation is substantially higher than reported previously.[9] One reason for the large signal may be the greater acceptance angle of the photodiode compared to a microscope objective. Since the cross section of the photodiode is relative large (50 μm^2) and the source of light scattering is probably a small submicron asperity at the end of the cantilever, the resulting acceptance angle may approach 180°.

Near-field imaging was conducted on two samples, a polycarbonate grating used for compact disk calibrations and a clean glass prism. In each case the sample was first imaged in conventional repulsive mode AFM and then the same area

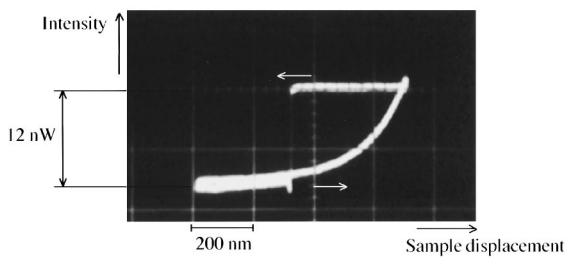

FIG. 4. Evanescent light intensity detected with the photocantilever as a function of sample displacement.

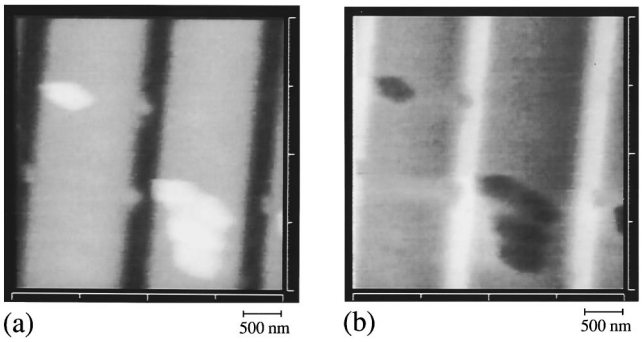

FIG. 5. AFM topographic image of a 1.6 μm period polycarbonate grating in contact mode (a) and the corresponding near-field optical image (b).

was imaged in SNOM mode without detaching the cantilever from the surface. The AFM image was taken in constant force mode. The SNOM image was taken without feedback with typical optical signal levels of 2 to 5 nW. AFM and SNOM imaging was not conducted simultaneously since the diode laser used for the AFM detection is within the bandwidth of the SNOM photodiode's sensitivity and, therefore, causes it to saturate. Simultaneous imaging will be possible by reducing the laser power for AFM detection and by depositing a metal layer on the back side of the cantilever for the optical shielding. The grating shown in the AFM image in Fig. 5(a) has a period of 1.6 μm and a step height of approximately 100 nm. A corresponding SNOM image is shown in Fig. 5(b). Many of the particles visible in the AFM image also appear on the SNOM image of which the smallest features are 120 nm particles. Figures 6(a) and 6(b) show contamination on the surface of the prism in AFM and SNOM modes, respectively. Five particles visible in the AFM image are also visible in the SNOM image. The smaller of the two particles near the center of the image measures 25 nm across and 30 nm in height. The vertical bars visible in the background of the SNOM image are caused by 50 Hz electrical noise coupling to the photodiode preamplifier.

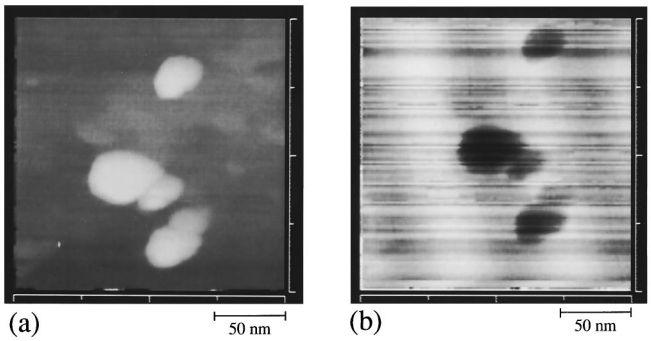

FIG. 6. AFM topographic (a) and the corresponding near-field optical (b) images of a glass prism surface. The scan area is 190 nm×190 nm.

We have fabricated and demonstrated the use of a photosensitive force-sensing cantilever for use in combination AFM and SNOM. The microfabricated device effectively miniaturizes an instrument configuration demonstrated by van Hulst *et al.*[9] The photocantilever has detected large optical signal levels of tens of nanowatts from evanescent fields. This efficiency is due in part to a larger collection angle than is possible using a conventional microscope objective. The fabrication process for the photocantilever can be combined with processes to make tips on the cantilever[6,14] as well as processes for making piezoresistive sensors[10] to create a combined SNOM and AFM needing no external optical detectors.

N. Yamauchi, A. Okamura, N. Kakuta, T. Yoshimura, and T. Usuda provided valuable microfabrication assistance. K. Fukuzawa made valuable suggestions regarding optics. The authors appreciate the encouragement of C. F. Quate. S.A. was supported by postdoctoral fellowships from the National Institute for Advanced Interdisciplinary Research and the NTT Interdisciplinary Research Laboratories.

[1] G. A. Massey, Appl. Opt. **23**, 658 (1984).
[2] U. Dürig, D. W. Pohl, and F. Rohner, J. Appl. Phys. **59**, 3318 (1986).
[3] D. Pohl, in *Scanning Tunneling Microscopy II*, edited by R. Wiesendanger and H. Güntherodt (Springer, Berlin, 1992), pp. 233–269.
[4] E. Betzig and J. K. Trautman, Science **257**, 189 (1992).
[5] J. A. Cline, H. Barshatzky, and M. Issacson, Ultramicroscopy **38**, 299 (1991).
[6] T. R. Albrecht, S. Akamine, T. E. Carver, and C. F. Quate, J. Vac. Sci. Technol. A **8**, 3386 (1990).
[7] E. Betzig, P. L. Finn, and J. S. Weiner, Appl. Phys. Lett. **60**, 2484 (1992).
[8] N. Chiba, H. Muramatsu, T. Ataka, H. Monobe, and M. Fujihara, Jpn. J. Appl. Phys. **34**, 321 (1995).
[9] N. F. van Hulst, M. H. P. Moers, O. F. J. Noordman, R. G. Tack, F. B. Segerink, and B. Bölger, Appl. Phys. Lett. **62**, 461 (1993).
[10] M. Tortonese, R. C. Barrett, and C. F. Quate, Appl. Phys. Lett. **62**, 834 (1993).
[11] J. Brugger, N. Blanc, Ph. Renaud, and N. F. de Rooij, Sens. Actuators A **43**, 339 (1994).
[12] S. Sze, *Physics of Semiconductor Devices* (Wiley, New York, 1981), pp. 750–751.
[13] W. P. Maszara and T. Thompson, J. Appl. Phys. **72**, 4477 (1992).
[14] S. Akamine, R. C. Barrett, and C. F. Quate, Appl. Phys. Lett. **57**, 316 (1990).